

Characteristic features of accelerated electrons on Lower Hybrid Current Drive experiments in the FT-2 tokamak

S.I. Lashkul, V.V. Rozhdestvensky, A.B. Altukhov, V.V. Dyachenko, L.A. Esipov, M.Yu. Kantor, D.V. Kouprienko, S.V. Krikunov, A.Y. Stepanov

A.F. Ioffe Physical-Technical Institute, Politekhnicheskaya 26, 194021, St.Petersburg

In Lower Hybrid Current Drive (LHCD) experiments in the tokamak FT-2 ($I_{pl} = (30 \div 35)$ kA, $\Delta t_{RF} = (5 \div 14)$ ms, $B_{tor} = 2.2$ T, $P_{RF} = (100 \div 150)$ kW, $F = 920$ MHz, $\lambda = 30$ cm) efficiency of the used two waveguide grill has been shown and main factors effecting on non inductive plasma current conditions was characterized [1]. The LHCD profile is defined by GRILL3D and FRTC code simulation on the base of plasma experimental data. Unfortunately it wasn't taken into account an influence of the residual

vortex electrical field on conditions of the non thermal electron ($E \sim (10 \div 100)$ keV) generation and their subsequent acceleration up to a few MeV which determines the non inductive plasma current. These circumstances together with experimental difficulties does not permit to interpret so far a row effects observed at HF power launching, particularly, suppression of MHD oscillations followed by plasma density rise. Measurements of the electron temperature profiles $T_e(r)$ performed by laser Thomson Scattering (TS) diagnostics has shown that at the HF pulse of $\Delta t_{RF} = 5$ ms duration the plasma column is cooled as a result of redistribution of the plasma current between

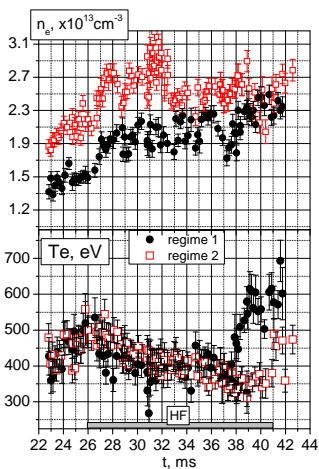


Fig.1 Changing of the density $n_e(y = 0\text{cm}, t)$ and temperature $T_e(y = 0\text{cm}, t)$ of the electrons for (a) regime 1 - $\langle n_e \rangle = 1.2 \times 10^{13} \text{ cm}^{-3}$ and (b) - regime 2 - $\langle n_e \rangle = 1.4 \times 10^{13} \text{ cm}^{-3}$

the base plasma OH current and a part of non inductive current of the runaway and accelerated electrons initiated by the LH wave (LHW). Non thermal electrons are generated by LHW with a parallel refractive index $N_{\parallel} \sim 1.8$. These experiments demonstrate the particles confinement time rise when ITB is formed near $r = (5 \div 6)$ cm. Cooling of the electron component is explained by that the thermalization time, t_{th} , of a non thermal electron beam in the plasma (t_{th} for $E_b \sim 0.2$ MeV is about $10 \div 15$ ms) is larger than the Δt_{RF} duration.

After the modulator modernization the HF pulse duration was increased up to 14 ms, that permits both to fulfill the effective additional heating of the electrons from 450 eV up

550÷600 eV and to reveal a row factors influencing on the LHCD efficiency. Dynamics of the electron density $n_e(y = 0\text{cm}, t)$ and electron temperature $T_e(y = 0\text{cm}, t)$ in the plasma column center during LHCD are shown in the Fig. 1. $T_e(r)$ profiles, appropriate to the beginning and end of the HF pulse for two experimental regimes, are presented in the Fig. 2. Regime 1, (Fig. 2a), is discharge with lower density where initial OH average density $\langle n_e \rangle = 1.2 \cdot 10^{13} \text{ cm}^{-3}$. Regime 2, (Fig. 2b), is discharge with $\langle n_e \rangle = 1.4 \cdot 10^{13} \text{ cm}^{-3}$. Here $y = 0 \text{ cm}$ is the coordinate of the vertical laser

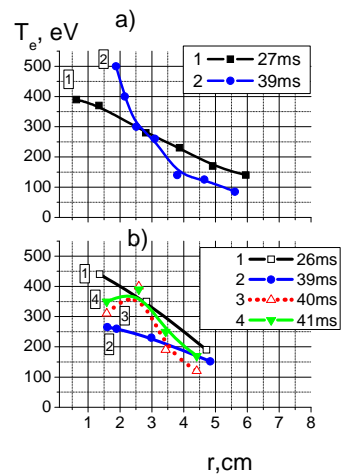


Fig. 2. Profiles $T_e(r)$ for the beginning (27ms) and end (39 – 41 ms) of the HF pulse for two experimental regimes. (a) Discharge with initial OH average density $\langle n_e \rangle = 1.2 \cdot 10^{13} \text{ cm}^{-3}$. (b) Discharge with $\langle n_e \rangle = 1.4 \cdot 10^{13} \text{ cm}^{-3}$

beam chord shifted outward along major radius R at 1.5 cm from the chamber center. Fig. 1 and Fig. 2 show that the fast rise of electron temperature during (2 ÷ 2.5) ms from 400 eV up (550÷600) eV after initial cooling is observed in the regime 1. For the regime 2 under of some larger plasma density the additional electron heating in the HF pulse end is observed at the region of 2 cm of the plasma cross-section. It is difficult to explain such fast heating by accelerated electron beam thermalization due to collisions with thermal plasma electrons.

To explain the additional electron heating effect the following facts were taken into account. Residual vortex electric field E_θ (Fig.3a) increases velocity of nonthermal electrons produced by the LH wave larger then critical value. After that they become runaways accelerated up to MeV - th energies. Microwave emission power measurements were fulfilled in the LHCD regime at low plasma density. It was done both with a collimated pyroelectric bolometer in the wavelength range $\lambda < 15\text{mm}$ (because of the diameter of the collimator is 8mm) and 4-, 2-mm heterodyne radiometers in frequency ranges appropriating to the magnetic broadening of the first and second electron cyclotron harmonics of thermal electrons. Essential increase of radiation losses due to significant synchrotron emission intensity growth during the HF-pumping pulse was observed in such conditions. Fig.3b shows the signal of the bolometer located on the central chord. One can see that radiation power calculated over all plasma volume in supposition of homogeneous distribution of radiation losses (see right axis scale) is approximately equals to the half HF-pumping power

$P_{rad} \sim 0.5 * P_{HF}$. The essential increase of the hard X-ray intensity (Fig. 3d) and energy U_{bol} , Fig. 3b, together with the synchrotron emission power rise in the frequency band

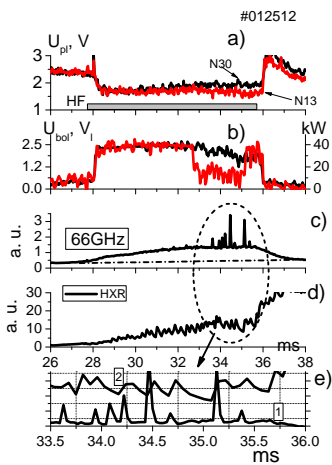


Fig. 3 Change of the plasma parameters during HF pulse. (a) The loop voltage $U_{pl} = 2\pi R E_\theta$. (b) – bolometric signal and radiation losses calculated from the bolometric signal. (c) synchrotron emission rise accompanied by spikes. (d) HXR signal. (e) Illustration of correlation of the spikes and HXR sawtooth shaped signals by faster scan. Red and black lines are two different shorts (N 13 and N 30).

this case. It was also shown that the runaway electron energy in vortex electric field acceleration is limited because of the significant synchrotron emission losses arising under resonance of gyromotion with the n -th harmonic of the toroidal magnetic field ripple.

Therefore large amount of accelerated electrons of limited energy, $W_{ripl}^{\max} = \frac{eBR_0}{nN\gamma m_0 c}$, is

accumulated in the plasma periphery forming the monoenergetic accelerated electron beam. Here: e , m_0 – charge and rest mass of an electron, γ – the relativistic gamma factor; B , R_0 , N – the toroidal magnetic field, major discharge chamber radius and number of toroidal magnetic coils, respectively [4]. When monoenergetic beam parameters are satisfied to the necessary and sufficient conditions for free electron microwave generation the CARM regime is realized. Such microwave generation arises as some following short spikes observed in the relatively narrow frequency band, [2, 3]. Fig. 3e shows a good correlation of these spikes with hard X-ray produced by local trapped accelerated electrons drifting on chamber walls.

The $\delta B = \Delta B_{tor} / B_{tor}$ value of the FT-2 magnetic ripple, $N = 24$, near the limiter reaches 10%. Therefore accumulation of accelerated electrons of limit energy, $W_{ripl}^{\max} \sim 3 \div 8$ MeV, [5], in the LH current drive (LHCD) regime with residual vortex electric field may

$\Delta f = (53 \div 156)$ GHz were registered. The significant synchrotron emission rise was accompanied by short microwave radiation spikes of another nature observed in the more narrow frequency band, $\Delta f = (53 \div 78)$ GHz, which is illustrated as example for 66 GHz in Fig. 3c. Such effect was earlier registered during plasma ohmic heating initial stage in the ASDEX-U tokamak, [2, 3]. These spikes appear due to interaction of accelerated electron beam with toroidal magnetic field ripple harmonics at the plasma periphery under the cyclotron auto resonance maser (CARM) conditions. The pitch angle of accelerated electrons, $\theta \sim v_\perp / v_\parallel$, increases and beam energy becomes isotropic in

provide not only growth of the powerful synchrotron emission in a broad frequency range but also the CARM amplification of synchrotron emission at appropriate frequencies. The frequency dependence of the relative increase of synchrotron emission power under the HF plasma pumping calculated for regime 1 in the beginning and end of HF pulse is presented in Fig. 4. One can see that it exhibits some wells at characteristic frequencies:

$$f_{Be} = \frac{1}{2\pi} \frac{ZeB}{m_e c} = 62 \text{ GHz}, \quad f_{Pl} = \frac{1}{2\pi} \sqrt{\frac{4\pi e^2 n}{m_e}} = 28 \text{ GHz}, \quad \text{for } n_e = 10^{13} \text{ cm}^{-3}, \quad f_{UHR} = \sqrt{f_{Be}^2 + f_{Pl}^2} = 68 \text{ GHz},$$

where f_{Be} , f_{Pl} и f_{UHR} – Electron Cyclotron Resonance, (ECR), plasma and Upper Hybrid Resonance, (UHR)/ frequencies.

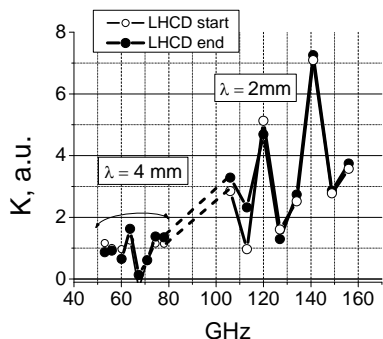


Fig. 4 Frequency dependence of the synchrotron emission power relative increment under the HF plasma pumping calculated for regime 1 in the start and end of HF pulse.

These facts indicate that at the LHCD regime effective absorption of synchrotron emission by thermal electrons is possible. As the powerful synchrotron emission spikes arise in the FT-2 tokamak together with the decrease of the loop voltage, bolometer signal and electron heating in the LHW-pulse end, Fig.3, one can suppose that the additional relatively fast central heating of electrons is due to the linear

transformation in the UHR region of the synchrotron emission extraordinary mode into the Bernstein waves which are absorbed then in the electron cyclotron resonance, ECR, region at frequencies $f \sim (60 \div 70)$ GHz ($\lambda = 4 \text{ mm}$), $B_{tor} = 1.95 \text{ T}$, [5]. Red and black lines in Fig. 3 illustrate the shorts with different additional electron heating effect during LHCD.

The study was fulfilled under support of grants RFFI 10-02-00631, 11-02-00561 and Russian Government Grant according to Ordinance No. 220 under Agreement No. 11.G34.31.0041 with Ministry of Education and Science of Russia.

References

- 1 S. I. Lashkul et al. Plasma Physics Reports, 2010, Vol. 36, No. 9, pp. 751–761
- 2 B. Kurzan K.-H. Steuer and W. Suttrop Rev. Sci. Instr. 68 (1). January 1997 P.423-426
- 3 B. Kurzan and K.-H. Steuer. PhysL Rev E. V55, N 4 (1994) P. 4608 – 4616
- 4 Z.Y. Chen et al. 21st IAEA FEC Chengdu, China 16 - 21 October (2006), EX/P3-4
- 5 V.N. Budnikov et al. Proc. of the 25th EPS Conf , Praha, 1998, P. 1360
- 6 V.E. Golant, V.I. Fedorov. High-Frequency Plasma Heating (A.G. Litvak, Ed.). American Institute of Physics, New York, 1992. Ch. 2..